# Optical assessment of nonimaging concentrators

Andreas Timinger, Abraham Kribus, Harald Ries, Toni Smith, and Markus Walther

An optical measurement method for nonimaging radiation concentrators is proposed. A Lambertian light source is placed in the exit aperture of the concentrator. Looking into the concentrator's entrance aperture from a remote position, one can photograph the transmission patterns. The patterns show the transmission of radiation through the concentrator with the full resolution of the four-dimensional phase space of geometric optics. By matching ray-tracing simulations to the measurement, one can achieve detailed and accurate information about the geometry of the concentrator. This is a remote, noncontact measurement and can be performed *in situ* for installed concentrators. Additional information regarding small-scale reflector waviness and surface reflectivity can also be obtained from the same measurement with additional analysis. © 2000 Optical Society of America

*OCIS codes:* 000.4430, 080.2740, 120.7000, 120.4290.

## 1. Introduction

Various applications, in particular solar devices, require a concentration of radiation. In cases in which information about the source is not required, the concentrator of choice may be a nonimaging device. Nonimaging concentrators have been proposed that have a performance often close to the thermodynamic limit.[1–3] However, the performance of real concentrators falls short of the theoretical prediction owing to inaccuracies in manufacturing, assembly, and alignment as well as imperfect reflectivity of the mirrors. Generally, it is difficult to assess the optical performance of the manufactured nonimaging concentrator from thermal measurements inside the receiver attached to the concentrator. Calorimetric measurements[4,5] and flux measurements[6] provide only limited detail and accuracy and offer no information on how the actual device geometry deviates from the design. We propose a method for determining the optical properties and the detailed actual geometry of a concentrator by using an all-optical measurement. The method is suitable for nonimaging devices in general, i.e., also for nonimaging illumination optics. We focus on concentrators without restricting generality.

The method is based on the reversibility of geometric optics. An ideal concentrator produces Lambertian radiation at its exit aperture; conversely, radiation from a Lambertian source placed at the exit aperture of a secondary concentrator will emerge through the entrance aperture, precisely with that phase-space distribution, which is accepted by the secondary, only with all direction vectors reversed. An observer looking into the entrance aperture will see patterns. These patterns characterize the transmission of radiation through the concentrator for the specific concentrator geometry. We photograph these patterns and hence measure the radiance distribution produced by the source and the concentrator. Photometric measurements of radiance distributions with four-dimensional resolution can be realized at a high automation level.[7,8]

The actual geometry of the reflective surfaces can be deduced from a comparison between the measured acceptance and a ray-tracing simulation. By changing the geometric parameters of the concentrator model used in the ray-tracing program, one could optimize the match between simulation and measurement. The set of geometric parameters yielding the best match would provide information on manufacturing and assembly errors of the concentrator relative to the original design.

The measurement procedure was applied to a secondary concentrator that was designed and constructed for a test station at the solar tower at the

A. Timinger and H. Ries are with Optics and Energy Concepts, Stoeberlstrasse 68, D-80686 Munich, Germany. A. Kribus is with the Department of Environmental Sciences and Energy Research (ESER), Weizmann Institute of Science, Rehovot 76100, Israel. T. Smith is with the National Renewable Energy Laboratory, Center for Buildings and Thermal Systems, 1617 Cole Boulevard, Golden, Colorado 80401. M. Walther is with Hugo-Troendle-Strasse 1, 80992 Munich, Germany.

Weizmann Institute of Science (WIS). We carried out the measurement in the laboratory rather than *in situ* to make sure that we had a controlled environment and adequate image resolution with standard optical equipment. Additional measurements on other concentrators were performed in situ and will be reported separately.

## 2. Principle

### A. Transmission Function

In the phase space of geometric optics, a ray can be described by four coordinates. Two coordinates denote the intersection point of the ray and an appropriate reference surface. Two coordinates denote the direction of the ray relative to the surface.[1,9] Radiation fills a volume in this phase space. The transmission of radiation coming from a source passing through an optical system is a function within this four-dimensional phase space that maps one volume (the source radiation) into another volume (the radiation at the target). For energy transfer it is of interest only which fraction of the radiant power of an incoming ray is transmitted to the target. We call this fraction the transmission function. It has values in the range between zero and one. This function is unique for each optical system. Every change in the geometric or optical properties of the system must affect the transmission of at least part of the radiation in the considered phase space volume. Hence the full transmission function represents a complete characterization of the optical system. A common measurement of concentrators consists of measuring the flux at the entrance and exit apertures. This condenses the transmission function on a two-dimensional subspace, because the flux measurement constitutes an integral over the directional extent of the radiation. Owing to loss of information, the geometry of the concentrator cannot be uniquely reconstructed from a flux measurement. Another common option is a calorimetric measurement: This collapses all transmission information into a single scalar and therefore provides even less information than a flux measurement. The proposed optical measurement method is designed to assess the transmission function through a nonimaging device with a full four-dimensional resolution, i.e., without integrating within subspaces.

### B. Transmission Patterns

A way to visualize the transmission function in a two-dimensional (2D) subspace is through the use of transmission patterns recorded as 2D images. The transmission function of rays coming from a given incident direction is plotted on the entrance aperture of an optical system. Rays that are transmitted to the exit aperture after a certain number of reflections fall on certain regions on the entrance aperture. Rays that are turned back after a certain numbers of reflections and are rejected through the entrance aperture intersect well-defined regions of the entrance aperture.[1] Both of these regions form a pattern, as
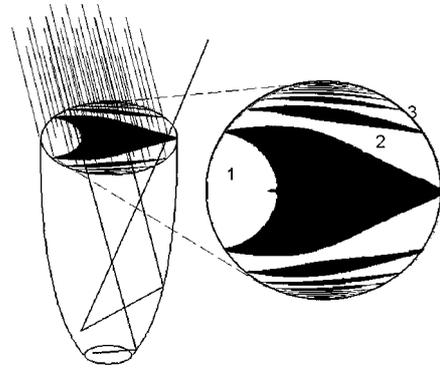


Fig. 1. Representation of the transmission function by transmission patterns. The rays are falling on the entrance aperture of a CPC with a 10° acceptance half-angle. Collimated radiation is incident at an angle of 10° to the CPC optical axis. One ray crosses the aperture within a dark region and is rejected through the entrance aperture after two reflections. The other ray crosses the entrance aperture through a light region and is transmitted to the exit aperture. The numbers in the light regions denote the number of reflections before transmission.

shown in Fig. 1, for a compound parabolic concentrator (CPC). Regions with ray rejection are black, regions with transmitted rays are blank with the number of reflections denoted.

In the case of collimated radiation a single transmission pattern shows the transmission function for the optical system in a 2D subspace, corresponding to the two spatial coordinates, for rays coming out of a constant direction. A series of observations from a dense set of locations allows a complete characterization; i.e., it yields all information of the full four-dimensional transmission function. It is not necessary that the observations be made from a great distance. Observation from a great distance[1] offers only the technical advantage that all regions of one pattern pertain to essentially the same direction. For short-distance observations, information for one direction may need information from several patterns. The principle amounts to exploring the shape of a four-dimensional object, the phase space of accepted radiation, by making cross sections with a series of 2D manifolds, the transmission patterns. It is only a technical issue that for transmission patterns from close up these 2D manifolds do not constitute planes parallel to two coordinate axes.

### C. Measurement Principle

The measurement method for the transmission patterns is based on the reversibility of the path of a ray in the framework of geometric optics. We place a Lambertian source of radiation at the exit aperture of the concentrator producing the radiation that is accepted by the concentrator but with reverse direction, hence reversing the optical path of the radiation. Looking onto the entrance aperture of the concentrator, one can see a pattern of bright regions enlightened by the Lambertian source and dark regions where radiation is absent. One directly observes the transmission pattern for those rays that intersect the

position of observation. A series of photographs from a dense 2D network of positions provides all the information about the transmission function.

Harper *et al.*[10] used a similar method in which light reflected at a certain angle is measured by a photocell. In contrast to this research in which each measurement produced one number, our observation yields a picture, i.e., a pixel array of brightness values. Each of these can be assigned to a differential phase space around a well-defined optical path. This path for each pixel can be inferred by knowing the position of observation, the focal length of the imaging camera, and the size of the film (or CCD sensor). Granted, for close-up observer locations the direction of the optical path connected with each pixel is not the same; nevertheless this constitutes no loss of information. Therefore it is not essential to record the transmission patterns from a great distance as in the case in Ref. 10. However, practical considerations sometimes suggest observing the transmission patterns from particular locations. In general, taking the transmission pattern photographs from the same location as the radiation source, for which that particular concentrator is designed, offers the advantage of yielding the optical efficiency for the particular position within the source through direct integration.

## 3. Measurements on a Concentrator with a Pentagonal Cross Section

A test series of photographs was taken at the WIS. The measurements were made in a laboratory with the concentrator mounted on an optical bench. The laboratory was darkened to reduce all light other than the Lambertian source of radiation.

### A. Concentrator

In this test we analyzed a nonimaging secondary concentrator that is part of an array of secondary concentrators for a partitioned receiver system at the WIS solar tower.[11,12] The concentrator is designed for the final concentration of radiation at the rim of the focal spot of a group of heliostats. The concentrated radiation is fed into the intermediate temperature stage (750 °C) of the partitioned receiver.

The concentrator is constructed from 15 facets. The facets are arranged in 3 rings of 5 facets, each ring having a pentagonal cross section in the plane perpendicular to the axis of the concentrator. The first two rings, starting from the exit aperture, consist of 5 plane facets each. The third ring consists of facets with one-dimensional parabolic curvature along a cross section containing the axis. This geometry is an approximation of a CPC that concentrates radiation from a 12° entrance angle. The chassis of the first two rings is made from solid pieces of aluminum with internal channels for water cooling. The chassis of the curved facets are made from aluminum sheets ground to parabolic shape. Thin backsurface glass mirrors are glued to the chassis with a thin adhesive film that can conduct the heat from the mirrors to the chassis. Figure 2 shows the
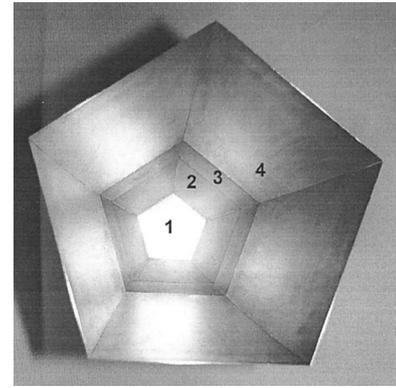


Fig. 2. Pentagonal concentrator before the mirrors are glued to the chassis. Starting from 1, the pentagonal exit aperture, one can distinguish 2 and 3, the two rings of plane facets, and 4, the parabolic sheets.

geometry of the concentrator.

### B. Experimental Setup

The experiment was assembled on an optical table. The concentrator was assembled with a pentagonal holder that clamps the facets against one another. (In the solar receiver setup, leaves from adjacent concentrators support one another, and the external leaves are supported by a front plate.) The holder orients the pentagon so that it is symmetric about a horizontal plane (see Fig. 3). The concentrator was placed at one corner of the table, a laser was set at the other end of the table in front of the entrance aperture, and a camera was installed on a ruler that allows motion perpendicular to the line connecting the laser and the concentrator.

The laser was used to determine the optical axis of the concentrator. We installed a flat mirror at the exit aperture of the concentrator, which is perpendicular to the optical axis of the concentrator. The laser beam was aimed to the center of the exit aperture.
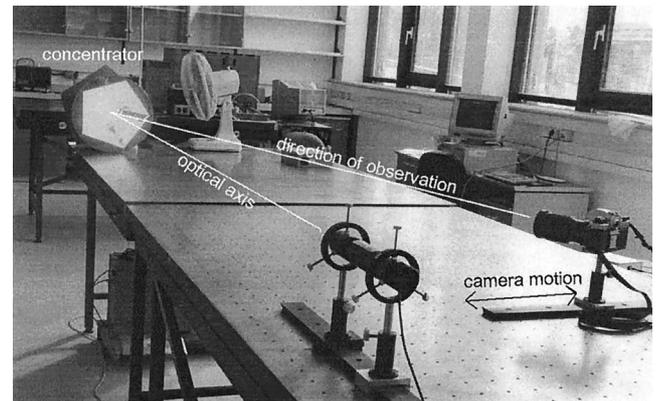


Fig. 3. Measurement system: the secondary concentrator, the laser used for alignment of the optical axis, and the camera. The axial distance between the concentrator's entrance aperture and the camera is 2.71 m. The maximal lateral displacement from the axis was 0.65 m. The outer diameter of the entrance aperture is 0.335 m.

The concentrator was moved and rotated until the position was reached at which the beam was reflected on itself. The optical axis of the concentrator was then the line connecting the center of the aperture to the laser.

The Lambertian light source consisted of a halogen lamp and several diffusing layers including cloth and plastic sheets. We used a semitransparent (milky white) plastic layer and three sheets of thick yellow cloth. Air gaps between the layers facilitated cooling and reduced the effects of the inhomogeneity in the cloth-layer density. The lamp emitted a considerable amount of heat, and a fan was used for active cooling of the lamp and the diffusing layers.

The spatial distribution of the light source was observed through the inlet aperture. Small-scale nonuniformity was observed that was due to density fluctuations in the cloth. However, on a scale larger than these small fluctuations, the brightness appeared uniform. The directional distribution was tested in both the vertical and the horizontal axes of symmetry of the halogen lamp by use of a fiber-optic minispectrometer. There is little variation in brightness at angles as large as 40° relative to the normal direction. Even at large angles of ~70°, the relative variation is ~20%. We may consider therefore the light source to be reasonably close to Lambertian.

The camera was moved along the ruler to eight different locations, where pictures of the transmission patterns were taken. The distance between the camera position and the optical axis was measured to determine the angle relative to the optical axis. The positions were chosen to yield angles as large as 18° relative to the optical axis (where nominal acceptance of the concentrator was 12°). After all eight pictures were taken, the process was repeated with the camera moving in the opposite direction.

## C. Transmission Patterns

Figure 4 shows six photographs of transmission patterns taken from different positions. Figures 4(a)–4(c) were taken from the left side of the optical axis when one is looking toward the concentrator. Figures 4(d)–4(f) were taken from the right side. The camera was relatively close to the concentrator; therefore the photographs do not represent transmission patterns of collimated radiation where each point pertains to the same direction. In our photographs the direction of the radiation varies within the entrance aperture. In Fig. 4 the ray direction varies by ±4° of the angle.

In all the photographs in Fig. 4 we see the exit aperture as a bright pentagon. The observer can estimate the off-axis angle from the apparent displacement between the entrance aperture and the exit aperture. The thin gaps between the facets appear as black lines. They can be observed directly together with their reflected images in the mirror facets. Several regions with different brightness can be clearly distinguished within each photograph. Different brightnesses are caused by attenuation
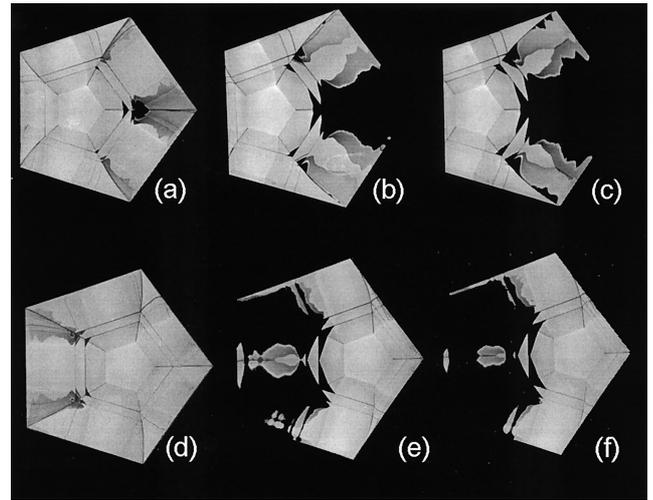


Fig. 4. Transmission patterns as seen from different positions of observation. Black regions correspond to rejected radiation. The first three photographs were taken from angles of (a) −5.3°, (b) −10.2°, and (c) −12.1° (to the left of the optical axis). The final photographs were taken from angles of (d) 6.0°, (e) 11.6°, and (f) 13.8° (to the right of the optical axis).

from different numbers of reflections. The reflectivity of the mirrors is 92–94%. The dark regions with no ray transmission become larger as the observer moves farther from the optical axis. In the patterns in Figs. 4(b), 4(c), 4(e), and 4(f) the dark regions extend to the rim of the pentagonal entrance aperture. All patterns in Fig. 4 should be symmetric with respect to the horizontal axis. Visible small deviations indicate imperfections in manufacturing and/or alignment of facets.

The area of the dark regions in the photographs measures the rejected radiation. This area can be quantified with standard image processing software. Figure 5 shows the complement of these values, i.e., the transmission for perfect reflectivity of the mirrors. The bars represent the spread of directions over one picture as seen from the position of observation. This spread is not equivalent to an error because it is strictly deterministic. Given a sufficient number of close-range photographs, one can calculate the transmission pattern for collimated light.

## D. Numerical Simulation

We simulated the transmission seen by the observer in the experiment by using ray-tracing software. Figure 6 shows a set of transmission patterns that compares experiment with simulation. Figure 6(a) shows the actual photograph. Figure 6(b) shows the simulation for the concentrator as designed. In the simulated pattern in Fig. 6(c) we added deviations to the nominal design shape to obtain a better match with the observed pattern in Fig. 6(a). First, the reflector facets were displaced along their normal vectors toward the optical axis to model the variability in the thickness of the adhesive tape used for gluing the mirrors to the supporting aluminum parts. This displacement allowed us to match the black
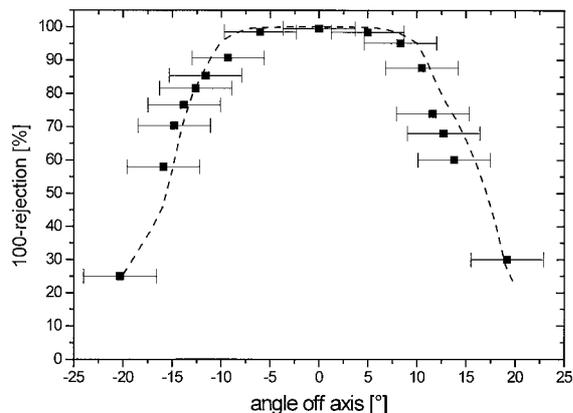
Fig. 5. Geometric acceptance, i.e., the compliment of rejection, as derived from the photographs. Horizontal bars illustrate the angular spread from the position of the observer. Negative angles correspond to radiation coming from a side of the entrance aperture; positive angles correspond to radiation coming from the edge of the aperture. Transmission of collimated radiation as obtained by ray-tracing simulations assuming the designed concentrator shape is shown by the dashed curve.

lines that appear in the two planar rings of the facets. Second, we varied the curvature of the parabolic sheets to match the general shape of the different patterns that appear on the parabolic leaves. Some of the features are highlighted by arrows in Fig. 6. We used a false-color representation to overlay simulation and measurement in one picture and thereby visually assess the quality of the match.

A facet displacement of as little as 0.25 mm could be visualized by some features of the patterns, e.g., the triangular dark regions in the sections with the plane facets. Compared with the total length of the concentrator of 37.5 cm, this translates to an accuracy of less than $10^{-3}$. The achievable accuracy is mainly limited by the resolution of the scanned picture and the imaging quality. We used one ray per pixel in the simulation. The resolution used for Fig. 6 was 290 × 310 pixels.

The oscillation of the transition between the dark region and the illuminated region can be matched with a slowly varying curvature of the sheets. These oscillations show an undesired waviness of the reflective surface on a length scale of centimeters.
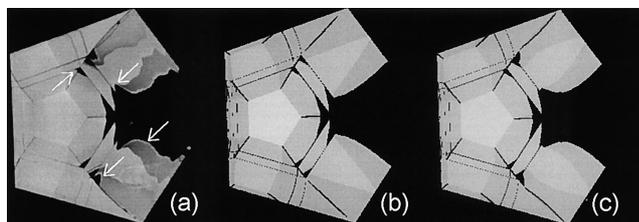


Fig. 6. Three transmission patterns as seen from 11.5° left of the optical axis: (a) photograph taken in the laboratory, (b) simulation of concentrator as designed, (c) simulation of the concentrator with added variations of shape for a better match with (a). The arrows highlight features that are better reproduced in (c) compared with (b).

A rigorous quantitative assessment of manufacturing errors is beyond the scope of this paper. It would be possible, however, along the lines discussed here by performance of a numerical optimization in a high dimensional space. This optimization can be based on a relatively small set of selected photographs. This is possible because each photograph contains a large amount of information. Photographs should preferentially feature both rejection and transmission; i.e., they should be taken from the transition region.

## 4. Conclusions

We have presented a noncontact optical method, based on reversing the optical path, for the assessment of nonimaging optical concentrators. A Lambertian source is placed at the exit aperture of a concentrator. Photographs of the transmission patterns of radiation emanating through the entrance aperture were taken from different positions. Each transmission pattern contained a vast amount of information. It visualized a 2D cross section through the four-dimensional phase space of geometric optics. With a set of pictures the transmission function can be assessed in four dimensions. The transmission patterns were also simulated by ray tracing.

A comparison of photographs with the simulated transmission patterns is a powerful diagnostic tool for the quality assessment of manufactured nonimaging devices. A test series for the optical analysis method showed the high accuracy in geometric parameters that can be obtained. A numerical optimization could include more parameters and model manufacturing tolerances in detail.

Our method does not require access to, or manipulation of, optical surfaces. The method can therefore be applied *in situ*, i.e., with the concentrator set up in its final position and the measurement performed from a remote position, for example, near the radiation source. For a primary concentrator with a long focal length, e.g., a field of heliostats, lenses with long focal lengths are required. It is essential to account for ambient light when pictures are taken outdoors. In addition to the laboratory measurements reported here, we have performed an *in situ* field measurement of a novel secondary concentrator designed for a field of heliostats. We plan to report this measurement in a forthcoming paper.

The method is suitable for nonimaging optical devices in which radiation coming from the same position can undergo different numbers of reflections before being transmitted to the exit aperture. This method complements other methods that are deployed for large-scale imaging concentrators such as photogrammetry.[13]

able suggestions and discussions and Chaim Barak for the high-quality photographs.

## References

1. W. T. Welford and R. Winston, *High Collection Nonimaging Optics* (Academic, New York, 1989).
2. R. P. Friedman, J. M. Gordon, and H. Ries, "Compact high-flux two-stage solar collectors based on tailored edge-ray concentrators," Sol. Energy **56,** 607–615, 1996.
3. A. Rabl, *Active Solar Collectors and their Applications* (Oxford University, Oxford, 1985).
4. A. Kribus, M. Huleihil, A. Timinger, and R. Ben-Mair, "Performance of a rectangular secondary concentrator with an asymmetric heliostat field," Sol. Energy **69** (in press).
5. D. Suresh, J. O'Gallagher, and R. Winston, "Thermal and optical performance test results for compound parabolic concentrators (CPCs)," Sol. Energy **44,** 257–270 (1990).
6. R. Buck, M. Abele, J. Kunberger, T. Denk, P. Heller, and R. Lüpfert, "Receiver for solar-hybrid gas turbine and combined cycle systems," in *Solar Thermal Concentrating Technologies*, G. Flamant, A. Ferriere, and F. Pharabod, eds., J. Phys. IV **9,** 537–544 (1998).
7. D. R. Jenkins and H. Mönch, "Source imaging goniometer method of light source characterization for accurate projection system design," in *Society for Information Display* (*SID*) *Symposium 2000, Long Beach, Calif.* (SID, San Jose, Calif., 2000), pp. 862–865.
8. R. F. Rykowski and C. B. Wooley, "Source modeling for illumination design," in *Lens Design, Illumination, and Optomechanical Modeling*, R. E. Fisher, R. Johnson, R. C. Juergens, W. J. Smith, and P. R. Yoder, eds., Proc. SPIE **3130,** 204–208 (1997).
9. M. Born and E. Wolf, *Principles of Optics* (Pergamon, Oxford, 1993).
10. A. Harper, R. Hildeband, R. Stiening, and R. Winston, "Heat trap: an optimized far infrared field optics system," Appl. Opt. **15,** 53–60 (1976).
11. P. Doron and A. Kribus, "Receiver partitioning: a performance boost for high-temperature solar applications," in *Eighth Symposium on Solar Thermal Concentrating Technologies, Cologne, Germany, 1996*, M. Becker and M. Böhmer, eds. (C. F. Müller, Heidelberg, 1996), Vol. 2, pp. 621–629.
12. A. Kribus, P. Doron, J. Karni, R. Rubin, E. Taragan, and S. Duchan, "Multistage solar receivers: the route to high temperature," in *Proceedings of International Solar Energy Society Solar World Congress, Jerusalem, Israel, 1999* (International Solar Energy Society, Freiburg, Germany, 2000).
13. M. Shortis and G. Johnston, "Photogrammetry: an available surface characterization tool for solar concentrators, part II: assessment of surfaces," J. Sol. Energy Eng. **119,** 286–291 (1997).